

Supercritical CO₂ aided polyindole-graphene nanocomposites for high power density electrode

Harish Mudila^{1,2}, Sweta Rana¹, Mohammad G. H. Zaidi^{1*}

¹Department of Chemistry, G. B. Pant University of Agriculture and Technology, Pantnagar, Uttarakhand, 263145, India

²Department of Chemistry, Lovely Professional University, Phagwara, Punjab, 144411, India

*Corresponding author. Tel. +919411159853; E-mail: mghzaidi@gmail.com

Received: 05 August 2016, Revised: 23 October 2016 and Accepted: 22 November 2016

DOI: 10.5185/amlett.2017.7018

www.vbripress.com/aml

Abstract

A series of Polyindole/Graphene nanocomposites (PGNCs) as electrochemical energy storage materials were fabricated at varying concentration (% w/w) of graphene ranging 3.0–9.0 in Polyindole (PIN) matrix in Supercritical CO₂. The electrochemical behavior of PGNC prepared at different proportion of graphene was investigated. The PGNC@9% has rendered specific capacitance of 389.17 F/g, along with energy and power densities of 13.51 Wh/kg and 511.95 W/kg respectively, which is greater as compared to graphene prepared through thermal reduction of graphene oxide. However, PIN comprises low capacitance of 24.48 F/g. Successive scans of PGNCs electrode for 1000 cycles at the scan rate of 0.1 V/s in KOH (1.0 M) shows a capacitive retention of ~98.6% indicating the electrochemical stability of the electrodes, with successive charge-discharge behavior. PGNCs display all the major peaks in Fourier Transform-Infrared and X-Ray diffraction spectra. Scanning electron micrograph in permutation with XRD spectra indicates the exfoliation of graphene into the matrix of PIN. Simultaneous TG-DSC reveals increased thermal stability of PGNCs with fractions of graphene. The good capacitive and charge-discharge performance indicates that supercritically fabricated PGNCs may serve as potential electrode materials for electrochemical energy storage devices. Copyright © 2017 VBRI Press.

Keywords: Graphene, nanocomposites, polyindole, scCO₂, specific capacitance, sulphonated polysulphone.

Introduction

The escalating industrialization and depletion of fossil fuel reservoirs has recently intensified the pursuit for the materials which can be projected as potential candidate for next generation energy storage devices [1, 2]. The stored energy under these energy storage devices is required to be delivered comprehensively with high current whenever needed, which is feasible only with high power density devices like supercapacitors. In this context, electrochemically active polymer nanocomposites (PNCs) derived through infusion of carbonaceous nanofillers into a variety of conducting polymers has recently been of special concern for development of electrochemical supercapacitors [3-7]. The improved electrochemical supercapacitance, reduced over-potential along with high rates of charge-discharge and extended cyclic stability are the principal attributes of such prepared PNCs [8, 9]. In this framework in last one decade and so, graphene due to its ease of preparation, low cost, high surface area, electrochemical activity, chemical stability and other assets exhibit great potential as filler for organic

conducting polymers viz. Polyaniline [4, 10], Polypyrrole [11-15] etc. for development of next generation electrochemical energy storage systems [16-18]. Such PNCs enabled enhanced electrochemical supercapacitance which reduced the over potential at high charge-discharge rate [5, 7].

Synthesis of PNCs involving carbonaceous nanofillers suffers Van der Waals interaction that limits their dispersion into polymer matrix. In this perspective, the significance of supercritical fluids, particularly supercritical carbon dioxide (scCO₂) as a green friendly alternative to organic solvents for dispersion of carbonaceous nanofillers into polymer matrix has recently been recognized greatly. This has been adopted either to develop the new technologies or to substitute the traditional technologies based on the use of organic solvents. The advantages of using scCO₂ over conventional methods for processing of PNCs are not only environmental but also chemical and economical [19-22]. scCO₂ is a smart solvent due to its critical temperature (T_c= 31.1°C) and moderate critical pressure (P_c=7.38 MPa) which allows simple removal of redox wastes by venting the pressure. In

the course to achieve high power density supercapacitors, $scCO_2$ assisted polymerization has emerged as an efficient tool, which not only offer a feasible and promising solvent free green approach alternative beyond traditional solvents polymer synthesis [23] but also endorses fuel cells [24] and improved capacitive energy storage materials [25, 26].

Polyindole (PIN) is one of the least studied polymer among polymeric electrochemical materials for electrochemical energy might due to its low level of electrical properties [27-31] which could be a consequence of low conductivity of PIN, this hinders the charge transfer within and to the contiguous PIN units, however *Mudila et al. 2014* had observed good level of specific capacitance for PIN with concentration of GO, which had inspired authors to investigate PIN in combination with graphene for determination of supercapacitance of composites. In this investigation $scCO_2$ assisted synthesis of Polyindole/Graphene Nanocomposites (PGNCs) was executed through $FeCl_3$ (1.85×10^{-2} mol/dL) assisted chemical oxidative polymerization of Indole (1g, 8.54×10^{-3} mol) in presence of graphene (@3-9%, w/w) in $scCO_2$. This investigation demonstrates that PGNCs synthesized through insitu $scCO_2$ assisted polymerization technique provide high specific capacitance with progressive concentration of graphene into the matrix of the conducting polymer. The spectral, microscopic, and thermal assessments recommend the complete entanglement of filler in polymer matrix while supercapacitance behavior has been explored through cyclic voltammetry of the synthesized PIN and respective PGNCs in KOH (1.0 M). The synthesized PGNCs have shown their significance as a high power electrode material with stable supercapacitance up to 1000 cycles at a scan rate of 0.1 V/s. New and exciting results were observed with increasing concentration of graphene in the matrix of PIN, suggesting its significance as a potential candidate for future generation energy strategies.

Experimental

Starting materials

Indole (>99%), Polysulfone (Mw; 16×10^3), Chlorosulfonic acid (>99%) and graphite were purchased from Sigma Aldrich. Other chemicals and solvents were obtained from sd. Fine Chemicals India.

Preparation of thermally reduced graphene

Graphene Oxide (GO) was prepared by applying modified Hummers method based on oxidation of

graphite powder (average particle size 500 nm) as described [30]. The GO thus prepared was further reduced thermally into graphene, [32, 33] the deposited GO material was placed in a vacuum furnace (Optics India), which was evacuated by a roughing pump. The sample was introduced in the furnace at room temperature and pumped down, the furnace temperature was ramped up to 400 °C in 1 h, held at 900 °C for 2 h, and then brought down to room temperature in next 4 h.

Preparation of SPS

Sulphonated polysulphone (SPS) used as binder and one of the ingredients in the matrix was synthesized through sulfonation of polysulfone (PS) with chlorosulfonic acid in dichloromethane (DCM) as described [34]. The precipitated polymer was washed repeatedly with distilled water to remove traces of solvent and volatiles until neutral water was obtained, SPS thus prepared was dried overnight (80°C).

Synthesis of PGNCs

The recipe for Polyindole/Graphene Nanocomposites (PGNCs) was designed by dispersion of graphene (3-9%, w/w) into mixture of Indole (1g, 8.54×10^{-3} mol) and $FeCl_3$ (1.85×10^{-2} mol/dL) under nitrogen and was conducted in a stainless steel high pressure reactor (100 cm³), model MC 10 10 SI ST equipped with a PID temperature controller, manufactured by Pressure Products Industries, Warminster, Penn., USA. CO_2 (99.98 %) was delivered directly to the reaction cell at the desired pressure of 1800 psi and then heated at 90°C for 6h with an electrical heating tape wrapped around exterior of cell to execute the polymerization reactions under supercritical conditions therein. The temperature ($\pm 1^\circ C$) inside the cell was measured by thermocouple provided and displayed on PID temperature controller. While maintaining mechanical agitation the products were isolated through venting the CO_2 into DCM from the reactor cell at 40°C and 50 psi/min. The crude products were subsequently washed with methanol to remove the untreated monomer and initiator. Similar scheme was assumed to synthesize PIN in ~90% yield.

Fabrication of electrodes

The commercially available 316-SS was prepared to 1 cm² area and finished with an emery paper (mesh size 320600). It was then de-greased with acetone and subjected to surface oxidation at $50 \pm 1^\circ C$ for 1h. As prepared SPS was used as an effective binder for material. Electroactive material (65 mg) along with graphite (10 mg) was added to a solution of SPS (5 g/dL) in N-methyl Pyrrolidone (NMP). The

contents were ultrasonicated over 15 min. The solution (50 μL) was applied over SS substrate; this has afforded the cathodes with mass thickness of electroactive materials by 5 ± 1 mg over 316-SS substrate. The treated substrate was initially dried at room temperature for 2h, followed by $100^\circ\text{C}/400$ mm Hg for next 48 h.

Results and discussion

FT-IR spectra

FT-IR spectra of all samples were recorded on Thermo Nicolet FT-IR Spectrophotometer using KBr pellets (**Fig. 1a**). Raw graphite and GO revealed characteristic absorptions (cm^{-1}) as reported [35, 36]. GO has low level of conductivity and is less used as a conductive material as compared to graphene which is thermally stable and more electrically conducting. The reduction of GO to graphene significantly can furnish thermal stability and electrical conductivity, close to the level of graphite [32, 37]. FT-IR spectra for thermally reduced graphene oxide (900°C) is shown in **Fig. 1a(iii)**, indicates the removal of carboxyl groups and partial hydroxyl groups. Weak absorption peaks at ~ 1050 – 1150 cm^{-1} represent residual epoxide groups, and the peak exist at 1573 cm^{-1} is attributed to the aromatic C=C group, the graphene obtained at high temperature was improved with less dis-orderness [31]. The absorption peaks of PIN were in accordance with previous done work [38] (**Fig. 1a(iv)**). A representative PGNCs synthesized at 9.0 % w/w concentration of graphene shows characteristic absorption of PIN and graphene in its spectrum (**Fig. 1a(v)**).

XRD spectra of pulverized samples were recorded at room temperature over Rigaku-Geigerflex X-Ray Diffractometer using Cu-K α radiation. Debye-Scherrer formula was employed to estimate average particle size of all materials (Table 1) to confirm the nanostructure of PGNCs:

$$D = \frac{0.9\lambda}{\beta \cos \theta} \quad (1)$$

Where ' λ ' is wave length of X-Ray (1.541 \AA), ' β ' is FWHM (full width at half maximum), ' θ ' is the diffraction angle and ' D ' is particle size (diameter). The value of d (the interplanar spacing between the atoms) is calculated using Bragg's Law:

$$d = \frac{n\lambda}{2 \sin \theta} \quad (2)$$

Graphite and GO (**Fig. 1b(i) and (ii)**) shows peak in agreement with previously reported results [39-41]. The XRD pattern (**Fig. 1b(iii)**) of graphene achieved via reduction of GO, has a strong peak at $2\theta = 26.11^\circ$ (**Table 1**). In addition, the exfoliation of

GO sheets after rapid vaporization of the intercalated water molecules resulted severe modifications in interlayer distance of 7.47 to 3.41 \AA (**Table 1**) for GO and graphene.

Table 1. Grain size of all the fabricated material.

Material	2θ of the intense peak (deg)	θ of the intense peak (deg)	FWHM (β) of Intense peak Radians	Grain Size (D) nm	d-spacing (\AA)
GO	11.83	5.92	0.0045	30.68	7.47
Graphene	26.11	13.06	0.0084	17.00	3.41
PIN	24.49	12.25	0.0065	21.85	3.63
PGNC@3 %	24.10	12.05	0.0049	32.16	3.69
PGNC@6 %	23.94	11.97	0.0054	29.13	3.72
PGNC@9 %	23.74	11.87	0.0059	26.68	3.74

At various temperatures below 900°C the water molecules, the hydroxyl and the carboxyl groups are removed from GO and only few hydroxyl and epoxide groups were remaining [33]. XRD of PIN is observed in **Fig. 1b(iv)**, PIN shows $2\theta = 24.49^\circ$, $d = 3.63$ \AA [29]. With rise in concentration of graphene in the matrix of PIN, a regular increase in the gallery spacing of the PIN in respective PGNCs has been observed ranging 3.69 to 3.74 \AA with a shift in $2\theta = 24.10$ to 23.74° , such increase in the gallery spacing of PIN in the respective nanocomposites may be attributed to their lamination over monolayer graphene.

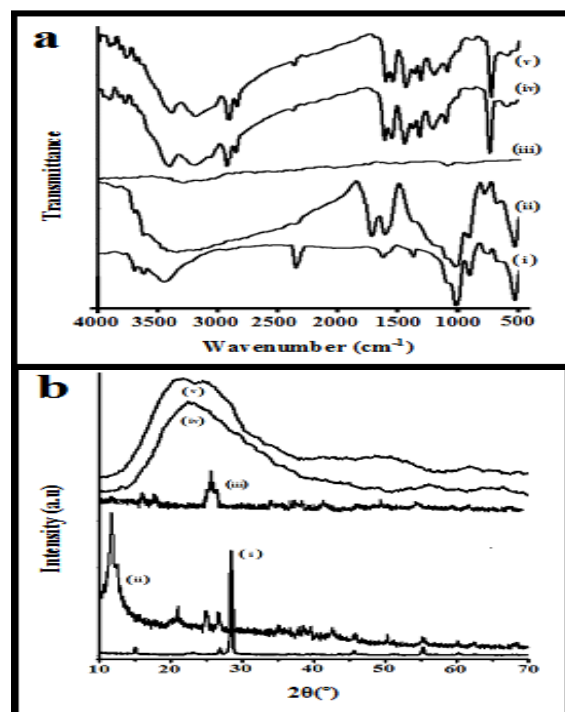


Fig. 1. (a) FT-IR and (b) XRD of Graphite (i), GO (ii), Graphene (iii), PIN (iv) and PGNC@9% (v).

XRD analysis

Moreover all the PGNCs have rendered characteristic diffused XRD spectra indicating their nebulous character. **Fig. 1b(v)** represents XRD pattern of PGNC@9.0 %, w/w of graphene.

Thermal analysis

TG of all the samples were recorded over TGA-50H with sample load ranging from 2.1 to 6.5 mg under inert N₂ atmosphere @ rate of 30 mL/min from ~20 °C to 600 °C. Thermal decomposition of PIN has been started with onset temperature (°C) 240.32 leaving residue (%) 91.44. Prior to onset temperature, the W_L (%) of 3.31 associated with PIN at 100°C was due to the trapped moisture [27, 44, 45]. The decomposition of PIN has been ended with endset temperature (°C) 599.72 leaving char residue (%) 10.36 (Fig. 2a). With concentration of graphene in the matrix, a gradual increase in the onset temperature (°C) of the respective PGNCs has been recorded ranging 312.09-442.28. The W_L (%) at 100°C corresponding to moisture content of PGNCs was ranging 1.05-0.85. While steady mass loss between 100 to 250°C is probably because of removal of residual oxygenated functional groups viz., CO and CO₂. 50% mass loss of active material ensues at ~560°C. For the composite there is mass loss in the range of 445 to 575°C due to decomposition of PIN and remaining functional groups which complete at 590°C. At onset temperature, PGNCs have left W_R (%) ranging 79.44-78.19. This has further been accompanied by a simultaneous increase in the endset temperature ranging 599.90-600 °C leaving char residue (%) ranging 42.11-58.18 (**Fig. 2a**). PIN and the respective PGNCs display rapid W_L (%) at temperature (°C) ranging 500-600 which was higher in case of PIN.

In order to have further insight into thermal stability of the electroactive polymer and respective PGNCs, their DSC scans were recorded over DSC-60 with a flow rate of 30 mL/min from ~25°C to 300°C (Fig. 2b). With concentration of graphene, the respective PGNCs have shown remarkable increase in the T_g ranging 53.11-71.81 °C. Such observations indicate respective PGNCs have shown higher thermal stability over PIN. The weak interaction and more ordered arrangement of the polymer and the graphene cause the regular increment in the T_g of PGNCs with concentration of active material, as compared to the electroactive polymer. The deflagration of graphene occurs at the high temperature, so in the case of PGNCs, the compact and ordered arrangements of graphene layers in the molecular chains of electroactive polymer functions as a barrier to heat passage, thus preventing the

deflagration of the polymer. The pronounced thermal stability implies that weak interaction and more ordered arrangement of the polymer and the active material (graphene) have caused the increment in the T_g temperature of composite [46, 47].

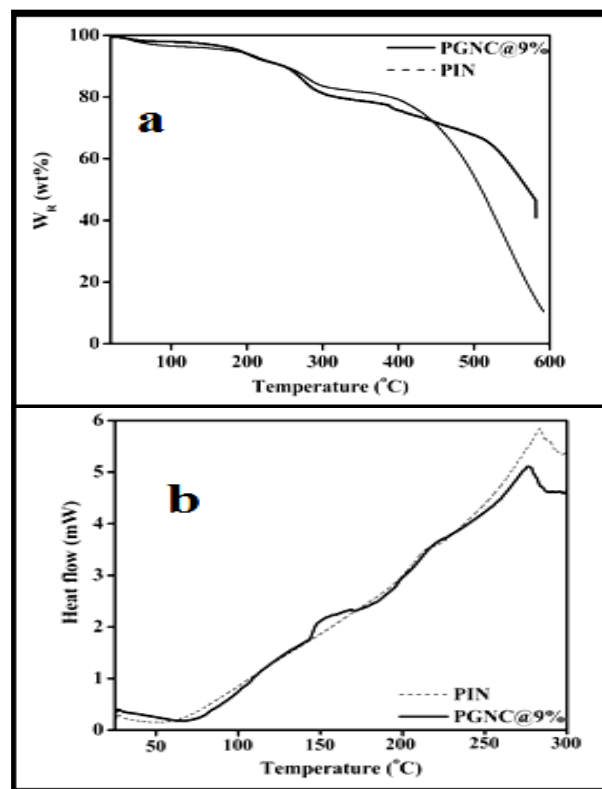


Fig.2. TGA (a) and DSC (b) curve of PIN and composite.

Electrochemical analysis

Electroactive nature of all the materials was observed with cyclic voltammetry (CV), scanned over IVIUM Potentiostat-Galvanostat Netherlands BV at current compliance 10 mA and ranges of voltage compliance -0.4 to 0.1 V, at scan rate (V/s) 0.001 to 0.15 using a three electrode cell assembly with reference to Ag/AgCl electrode. Pt foil with 1 cm² area was employed as counter electrode and commercially available 316-SS electrode as a working electrode. 1M KOH solution was used as electrolyte in whole experiment. All the materials represents CV closed to quasi rectangular shape, indicating the supercapacitive behavior of these materials. Electrochemical studies on graphene, PIN, and PGNCs, deliver us exciting outcomes which demonstrate PGNCs as quite efficient material for preparation and its development as a material for energy storage devices. Graphene has previously recognized to comprise of thriving capacity and a potential material to store energy. The CV were taken in the above said potential range at scan rates of 0.001 to 0.15 V/s, to provide specific capacitance of 241.30 to 3.361 (**Fig. 3a**).

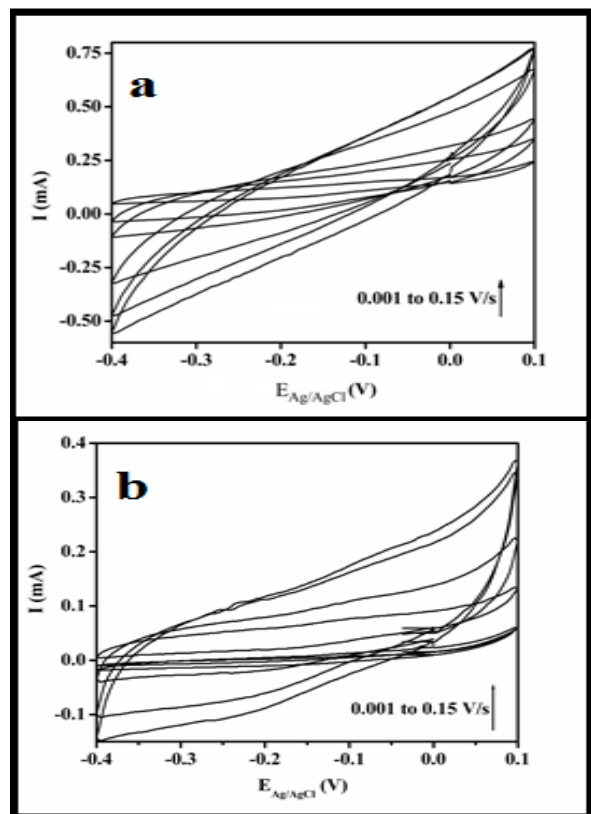


Fig. 3. CV of Graphene (a) and PIN (b) at various scan rates.

Specific capacitance (C_s) of the active materials was calculated from the voltammetric charges by the CV curve, by means of relation:

$$C_s = \frac{qa + |qc|}{2m\Delta V} \quad (3)$$

where, “qa” and “qc” are the voltammetric charges on anodic and cathodic scans, in the capacitive potential region (ΔV), and “m” being the mass of active material.

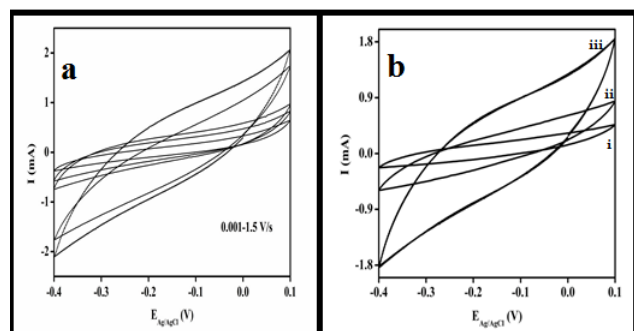


Fig. 4(a). CV of PGNC@9% at all scan rates (b) CV of PGNCs @3-9% (i-iii) at 0.01V/s.

PIN usually shows low level of electrochemical energy storage [48-50] as compared to graphene. PIN with increasing scan rate i.e. 0.001 to 0.15 V/s shows specific capacitance of 24.48 F/g to 1.75 F/g as observed in Fig. 3b. Fig.4a. demonstrates the

escalation in specific capacitance with scan rate for PGNC@9%. With increasing fraction of graphene (i.e. 3-9% w/w) in the matrix of polymer a steady increase was witnessed in the specific capacitance of PGNCs at 0.01V/s (Fig. 4b).

Fig. 5a. illustrate the comparative specific capacitance of graphene, PIN and PGNC@9% at scan rate of 0.001 V/s which demonstrate PGNC@9% to be most supercapacitive (389.17 F/g) which is comparable to the results achieved by previous researchers [49, 50] and PIN to be least capacitive of the all (24.48 F/g) which is further confirmed with the comparative histogram of C_s of all the electroactive materials (Fig. 5b). The increase in the capacitance of PGNC’s may be attributed to synergistic effects of the involved components, thus higher concentration of graphene imparts additional capacitance to the nanocomposites. On the contrary the decrease of capacitance with increasing scan rate in CV curves can be explained to the fact that, at a higher scan rate, charge diffusion is not able to follow the variation in electric field, and thus returns small capacitance or energy density values and high power density.

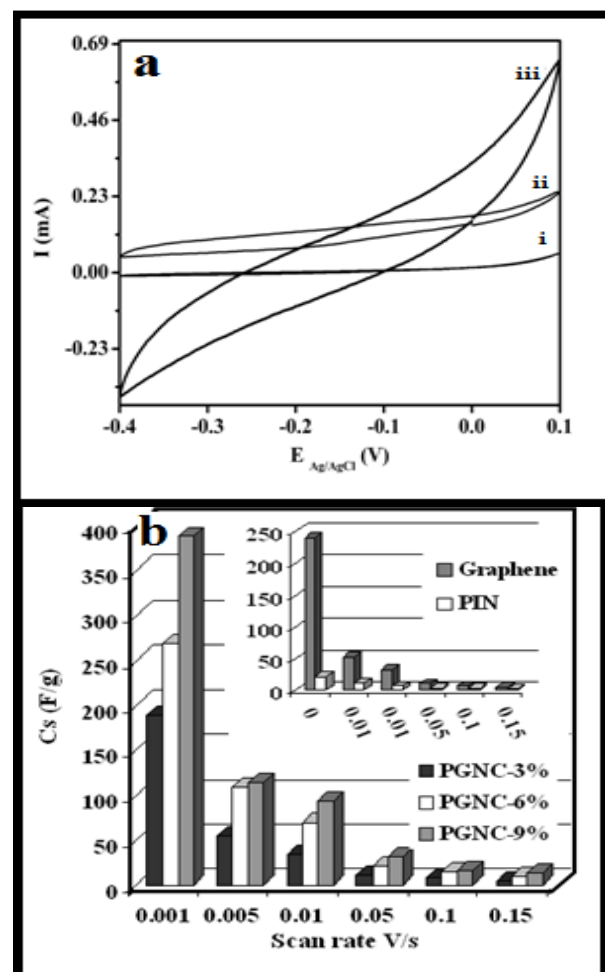


Fig. 5 (a). CV of PIN, Graphene and PGNC@9% (i-iii) at 0.001V/s (b) Specific capacitance of all electroactive materials.

The energy density (E) and power density (P) for PIN and NCs were estimated respectively through following equations:

$$E = \frac{Cs (\Delta V)^2}{2} \quad (4)$$

$$P = \frac{E}{\Delta t} \times 3600 \quad (5)$$

where, “Cs” is specific capacitance, ΔV is the applied initial voltage and “ Δt ” is the corresponding discharge time in hour, the maximum energy density of 1.00 Wh/kg and 13.51 Wh/kg for PIN and PGNC@9%, while corresponding power density of 36.00 W/kg and 511.95 W/kg was accounted for PIN and PGNC@9% respectively. These achieved power density was found to be much greater as compared to that power density obtained by Zhou *et al.* for PIN/RGO/CC electrode (500 W/kg at the energy density of 45 Wh/kg) and having comparable power density for V₂O₅/PIn/rGO and Graphene/CNT/PPY assembly [49-51]. This suggests that scCO₂ aides in achieving the higher level interaction of functional groups on PIN and Graphene which was advantageous to improve the specific capacitance of the prepared nanocomposites.

Fig. 6a. shows charging-discharging curves of PGNC@9% recorded in the voltage range from -0.4 V to 0.1 V at an applied current density of 10 mA/cm².

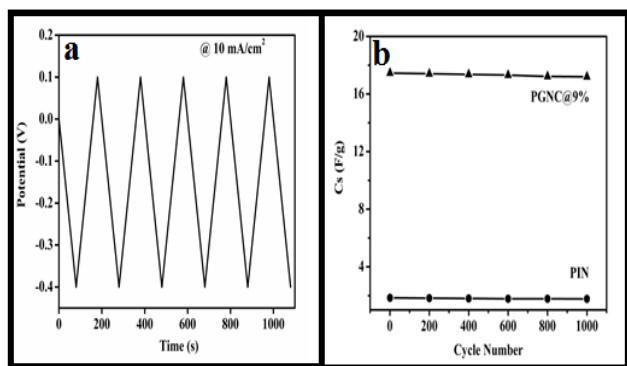


Fig. 6. (a) Charge-discharge curves for PGNC@9% (b) Effect of number of cycle on the Cs and stability.

The charge/discharge curves exhibit reversible characteristics without apparent deviation in each cycle, this charge/discharge curves are virtually linear in the total range of potential with constant slopes, representing perfect electrocapacitive behavior. This suggests good electrochemical stability for the PGNC electrodes. A ~98.6% capacitive retention through the first 1000 cycles at a 0.1 V/s, (Fig. 6b) indicates the excellent cyclic stability of the nanocomposites for supercapacitor applications.

Conclusion

A series of Polyindole-Graphene nanocomposites (PGNCs) were prepared through FeCl₃ assisted chemical oxidative polymerization of Indole in scCO₂. The FT-IR, XRD spectra and scanning electron micrographs reveals the formation of PGNCs. Simultaneous TG-DSC describes the thermal behavior of PGNCs which get more stable with percentage of graphene. CV studies suggest that these PGNCs having varying concentration of graphene (3-9%) in their matrix can be employed as potential material for the above said property. PGNC@9% had provided with specific capacitance of 389.17 F/g which is higher as compared to graphene, whereas PIN comprises of least capacitance of 24.48 F/g. A drop of ~1.4% in the specific capacitance of PGNCs electrode was observed for first 1000 successive cycles at the scan rate of 0.1 V/s, thus illuminating good cyclic stability of electrode material also the charge-discharge curves are almost linear in the total range of potential with constant slopes, presenting perfect electrocapacitive behavior. The maximum energy density of 1.00 Wh/kg and 13.51 Wh/kg was encountered for PIN and PGNC@9%, while corresponding power density of 36.00 W/kg and 511.95 W/kg was accounted respectively, which were found to be higher or comparable for the electrodes materials employed earlier for supercapacitive studies. The present efforts demonstrates an approach for synthesis of the electrochemically active PGNCs with improved capacitive, cyclic and galvanostatic charge-discharge behavior that may serve as potential candidate as electrode materials for development of electrochemical energy storage devices.

Acknowledgements

Authors are thankful for the financial assistance granted by Defence Research Development Organisation (DRDO) vide grant reference No.ERIP/ER/0703649/M/01/1092 and Department of Science and Technology (DST) Inspire fellowship No 110513.

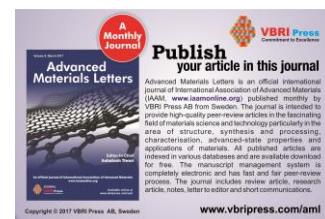
Author's contributions

Conceived the plan: HM, MZ; Performed the experiments: HM,SR; Data analysis: HM,SR, MZ; Wrote the paper: HM,SR, MZ.

References

- Vangari, M.; Pryor, T.; Jiang, L.; *J. Energy Eng.* **2013**, *139*, 72
DOI: [10.1061/\(ASCE\)EY.1943-7897.0000102](https://doi.org/10.1061/(ASCE)EY.1943-7897.0000102)
- Vlad, A.; Singh, N.; Rolland, J.; Melinte, S.; Ajayan, P. M.; Gohy, J. F.; *Sci. Rep.* **2014**, *4*, 4315.
DOI: [10.1038/srep04315](https://doi.org/10.1038/srep04315).
- Arico, A. S.; Bruce, P.; Scrosati, B.; Tarascon, J. M.; Schalkwijk, W. V.; *Nat. Mater.* **2005**, *4*, 366.
DOI: [10.1038/nmat1368](https://doi.org/10.1038/nmat1368)
- Wang, G.; Zhang, L.; Zhang, J.; *Chem. Soc. Rev.* **2012**, *41*, 797.
DOI: [10.1039/c1cs15060j](https://doi.org/10.1039/c1cs15060j)

5. Fang, Y.; Luo, B.; Jia, Y.; Li, X.; Wang, B.; Song, Q.; Kang, F.; Zhi, L.; *Adv. Mater.* **2012**, *24*, 6348.
DOI: [10.1002/adma.201202774](https://doi.org/10.1002/adma.201202774)
6. Ghosh, A.; Lee, Y. H.; *Chem. Sus. Chem.* **2012**, *5*, 480.
DOI: [10.1002/cssc.201100645](https://doi.org/10.1002/cssc.201100645)
7. Lu, P.; Xue, D.; Yang, H.; Liu, Y.; *Int. J. Smart and Nano Mater.* **2013**, *4*, 2.
DOI: [10.1080/19475411.2011.652218](https://doi.org/10.1080/19475411.2011.652218)
8. Wang, J.; Xu, Y.; Chen, X.; Du, X.; *J. Power Sources* **2007**, *163*, 1120.
DOI: [10.1016/j.jpowsour.2006.10.004](https://doi.org/10.1016/j.jpowsour.2006.10.004)
9. Sharma, A. K.; Kim, J. H.; Lee, Y. S.; *Int. J. Electrochem. Sci.* **2009**, *4*, 1560.
DOI: <http://www.electrochemsci.org/papers/vol4/4111560.pdf>
(last accessed on 23 October 2016)
10. Ramya, R.; Sivasubramanian, R.; Sangaranarayanan, M. V.; *Electrochim. Acta.* **2012**, *101*, 109.
DOI: [0.1016/j.electacta.2012.09.116](https://doi.org/10.1016/j.electacta.2012.09.116)
11. Mudila, H.; Rana, S.; Joshi, V.; Zaidi, M. G. H.; Alam, S.; *Int. J. Chem. Anal. Sci.* **2013**, *4*, 139.
DOI: [10.1016/j.ijcas.2013.09.001](https://doi.org/10.1016/j.ijcas.2013.09.001)
12. Shulga, Y. M.; Baskakov, S. A.; Abalyaeva, V. V.; Efimov, O. N.; Shulga, N. Y.; Michtchenko, A.; Lartundo-Rojas, L.; Moreno-R, L. A.; Cabañas-Moreno, J. G.; Vasilets, V. N.; *J. Power Sources* **2013**, *224*, 195.
DOI: [10.1016/j.jpowsour.2012.09.105](https://doi.org/10.1016/j.jpowsour.2012.09.105)
13. Sahoo, S.; Dhibar, S.; Hatui, G.; Bhattacharya, P.; Das, C. K.; *Polymer* **2013**, *54*, 1033.
DOI: [10.1016/j.polymer.2012.12.042](https://doi.org/10.1016/j.polymer.2012.12.042)
14. Lai, L.; Wang, L.; Yang, H.; Sahoo, N. G.; Tama, Q. X.; Liu, J.; Poh, C. K.; Lim, S. H.; Shen, Z.; Lin, J.; *Nano Energy* **2012**, *1*, 723.
DOI: [10.1016/j.nanoen.2012.05.012](https://doi.org/10.1016/j.nanoen.2012.05.012)
15. Wang, J.; Xu, Y.; Zhu, J.; Ren, P.; *J. Power Source.* **2012**, *208*, 138.
DOI: [10.1016/j.jpowsour.2012.02.018](https://doi.org/10.1016/j.jpowsour.2012.02.018)
16. Potts, J. R.; Dreyer, D. R.; Bielawski, C. W.; Ruoff, R. S.; *Polymer* **2011**, *52*, 5.
DOI: [10.1016/j.polymer.2010.11.042](https://doi.org/10.1016/j.polymer.2010.11.042)
17. Huang, Y.; Liang, J.; Chen, Y. Y.; *Small* **2012**, *8*, 1805.
DOI: [10.1002/sml.201102635](https://doi.org/10.1002/sml.201102635)
18. Taghioskoui, M.; *Mater. Today.* **2009**, *12*, 34.
DOI: [10.1016/S1369-7021\(09\)70274-3](https://doi.org/10.1016/S1369-7021(09)70274-3)
19. Brunner, G.; *Annu. Rev. Chem. Biomol. Eng.* **2010**, *1*, 321.
DOI: [10.1146/annurev-chembioeng-073009-101311](https://doi.org/10.1146/annurev-chembioeng-073009-101311)
20. Cooper, A. I.; *Adv. Mater.* **2003**, *15*, 1049.
DOI: [10.1002/adma.200300380](https://doi.org/10.1002/adma.200300380)
21. Zaidi, M. G. H.; Joshi, S.; Kumar, M.; Sharma, D.; Kumar, A.; Alam, S.; Sah, P.; *Carbon Lett.* **2013**, *14*, 218.
DOI: <http://dx.doi.org/10.5714/CL.2013.14.4.218>
22. Zaidi, M. G. H.; Thakur, A.; Agarwal, T.; Alam, S.; *Iran Polym J.* **2014**, *23*, 365.
DOI: [10.1007/s13726-014-0234-y](https://doi.org/10.1007/s13726-014-0234-y)
23. Soares da Silva, M.; Viveiros, R.; Coelho, M. B.; Aguiar-Ricardo, A.; Casimiro, T.; *Chem Eng Sci.* **2012**, *68*, 94.
DOI: [10.1016/j.ces.2011.09.015](https://doi.org/10.1016/j.ces.2011.09.015)
24. Bozbag, S. E.; Erkey, C.; *J. of Supercrit Fluids.* **2012**, *62*, 1.
DOI: [10.1016/j.supflu.2011.09.006](https://doi.org/10.1016/j.supflu.2011.09.006)
25. Xu, S.; Yang, H.; Wang, K.; Wang, B.; Xu, Q.; *Phys. Chem. Chem. Phys.* **2014**, *16*, 7350.
DOI: [10.1039/c3cp54957g](https://doi.org/10.1039/c3cp54957g)
26. Shenoy, S. L.; Cohen, D.; Weiss, R. A.; Erkey, C.; *J. Supercrit Fluids.* **2004**, *28*, 233.
DOI: [10.1016/S0896-8446\(03\)00047-0](https://doi.org/10.1016/S0896-8446(03)00047-0)
27. Rajasudha, G.; Shankar, H.; Thangadurai, P.; Boukos, N.; Narayanan, V.; Stephen, A.; *Ionics.* **2010**, *16*, 839.
DOI: [10.1007/s11581-010-0472-8](https://doi.org/10.1007/s11581-010-0472-8)
28. Trung, V. Q.; Huyen, D. N.; APCTP-ASEAN Workshop on Advanced Materials Science and Nanotechnology (AMSN08) IOP Publishing, *J. Phys.: Conference Series.* Vol. 187, 12058 **2009**.
DOI: [10.1088/1742-6596/187/1/012058](https://doi.org/10.1088/1742-6596/187/1/012058)
29. Gupta, B.; Chauhan, D. S.; Prakash, R.; *Mater. Chem. and Phys.* **2010**, *120*, 625.
DOI: [10.1016/j.matchemphys.2009.12.026](https://doi.org/10.1016/j.matchemphys.2009.12.026)
30. Mudila, H.; Rana, S.; Zaidi, M. G. H.; Alam, S.; *Fuller Nanotub Car N.* **2014**, *23*, 20.
DOI: [10.1080/1536383X.2013.787604](https://doi.org/10.1080/1536383X.2013.787604)
31. Stoller, M. D.; Park, S.; Zhu, Y.; An, J.; Ruoff, R. S.; *Nano Lett.* **2008**, *8*, 3498.
DOI: [10.1021/nl802558y](https://doi.org/10.1021/nl802558y)
32. Jung, I.; Vaupel, M.; Pelton, M.; Piner, R.; Dikin, D. A.; Stankovich, S.; An, J.; Ruoff, R. S.; *J. Phys. Chem. C.* **2008**, *112*, 8499.
DOI: [10.1021/jp802173m](https://doi.org/10.1021/jp802173m)
33. Tiwari, A.; (Eds), In the Graphene materials: Fundamentals and emerging applications, John Wiley & Sons, USA, **2015**.
34. Unnikrishnan, L.; Madamana, P.; Mohanty, S.; Nayak, S. K.; *Polym-Plast. Technol.* **2012**, *51*, 568.
DOI: [10.1080/03602559.2012.654580](https://doi.org/10.1080/03602559.2012.654580)
35. Thakur, S.; Karak, N.; *Carbon* **2012**, *50(14)*, 5331.
DOI: [10.1016/j.carbon.2012.07.023](https://doi.org/10.1016/j.carbon.2012.07.023)
36. Liu, K.; Li, Y.; Xu, F.; Zuo, Y.; Zhang, L.; Wang, H.; Liao, J.; *Mater. Sci. Eng.: C* **2009**, *29*, 261.
DOI: [10.1016/j.msec.2008.06.023](https://doi.org/10.1016/j.msec.2008.06.023)
37. Chen, W.; Yan, L.; *Nanoscale* **2010**, *2*, 559.
DOI: [10.1039/b9nr00191c](https://doi.org/10.1039/b9nr00191c)
38. Eraldemir, O.; Sari, B.; Gok, A.; Unal, H. I.; *J. Macromol. Sci. Pure.* **2008**, *45*, 205.
DOI: [10.1080/10601320701839890](https://doi.org/10.1080/10601320701839890)
39. Afanasov, I. M.; Shornikova, O. N.; Avdeev, V. V.; Lebedev, O. I.; Tendeloo, G. V.; Matveev, A. T.; *Carbon.* **2009**, *47*, 513.
DOI: [10.1016/j.carbon.2008.10.004](https://doi.org/10.1016/j.carbon.2008.10.004)
40. El Achaby, M.; Arrakhiz, F. Z.; Vaudreuil, S.; Essassi, E.; Qaiss, M. A.; *Appl. Surf. Sci.* **2012**, *258*, 7668.
DOI: [10.1016/j.apsusc.2012.04.118](https://doi.org/10.1016/j.apsusc.2012.04.118)
41. Wojtoniszak, M.; Chen, X.; Kalenczuk, R. J.; Wajda, A.; Łapczuk, J.; Kurzewski, M.; Drozdik, M.; Chu, P. K.; Borowiak-Palen, E.; *Coll. Surf. B.* **2012**, *89*, 79.
DOI: [10.1016/j.colsurfb.2011.08.026](https://doi.org/10.1016/j.colsurfb.2011.08.026)
42. Joshi, L.; Singh, A.; Prakash, R.; *Mater. Chem. Phys.* **2012**, *135*, 80.
DOI: [10.1016/j.matchemphys.2012.04.026](https://doi.org/10.1016/j.matchemphys.2012.04.026)
43. Goel, S.; Mazumdar, N. A.; Gupta, A.; *J. Nanosci. Nanotechnol.* **2011**, *11*, 10164.
DOI: [10.1166/jnn.2011.4993](https://doi.org/10.1166/jnn.2011.4993)
44. Abthagir, P. S.; Dhanalakshmi, K.; Saraswathi, R.; *Synthetic Met.* **1998**, *93*, 1.
DOI: [10.1016/S0379-6779\(98\)80125-2](https://doi.org/10.1016/S0379-6779(98)80125-2)
45. Abthagir, P. S.; Saraswathi, R.; *Thermochim. Acta* **2004**, *424*, 25.
DOI: [10.1016/j.tca.2004.04.028](https://doi.org/10.1016/j.tca.2004.04.028)
46. Zhou, J.; Yao, Z.; Chen, Y.; Xu, T.; Wu, Y.; *Society of Plastics Engineers.* **2013**, <http://www.4spepro.org/pdf/004998/004998.pdf>. Last accessed on 30 July 2016.
DOI: <http://www.4spepro.org/pdf/004998/004998.pdf>
47. Naebe, M.; Wang, J.; Amini, A.; Khayyam, H.; Hameed, N.; Li, L. H.; Chen, Y.; Fox, B.; *Sci. Rep.* **2014**, *4*, 4375.
DOI: [10.1038/srep04375](https://doi.org/10.1038/srep04375)
48. Giribabu, K.; Manigandan, R.; Suresh, R.; Vijayalakshmi, L.; Stephen, A.; Narayanan, V.; *Chem. Sci. Trans.* **2013**, *2*, 13.
DOI: [10.7598/cst2013.2](https://doi.org/10.7598/cst2013.2)
49. Zhou, Q.; Zhu, D.; Ma, X.; Xu, J.; Zhou, W.; Zhao, F.; *RSC Adv.* **2016**, *6*, 29840.
DOI: [10.1039/C5RA27375G](https://doi.org/10.1039/C5RA27375G)
50. Zhou, X.; Chen, Q.; Wang, A.; Xu, J.; Wu, S.; Shen, J.; *ACS Appl. Mater. Interfaces.* **2016**, *8*, 3776.
DOI: [10.1021/acsami.5b10196](https://doi.org/10.1021/acsami.5b10196)
51. Aphale, A.; Maisuria, K.; Mahapatra, M. K.; Santiago, A.; Singh, P.; Patra, P.; *Scientific Reports.* **2015**, *5*, 1.
DOI: [10.1038/srep14445](https://doi.org/10.1038/srep14445)



Supporting Information

SEM micrograph

Scanning micrographs of gold coated specimen derived from graphene, PIN and respective PGNCs were observed over JEOL (JSM-6610 LV) with beam voltage 5KV at 1.0 KX, 10 μ m shown in **Fig. S1(a-c)**. **Fig. S1a**. demonstrate SEM micrograph for thermally reduced graphene, it shows layered structure appear to corrugated into a wavy shape, closely associated with each other and forming a disordered solid. The surface of PIN electrode prepared in presence of SPS as binder has rendered the characteristic rod shaped grains of PIN, such rod shaped micro-domain formation has been the characteristic of PIN irrespective to their adopted method of synthesis [42, 43] (**Fig. S1b**).

with no distinct visibility of the microrods of the PIN. Such surface characteristic may be due to the formation of the PGNCs with intercalated domains of the PIN microrods among the entanglement space of the graphene as earlier observed through increase in the gallery spacing of GO due to the presence of PIN (in XRD spectra, **Fig. 1b**).

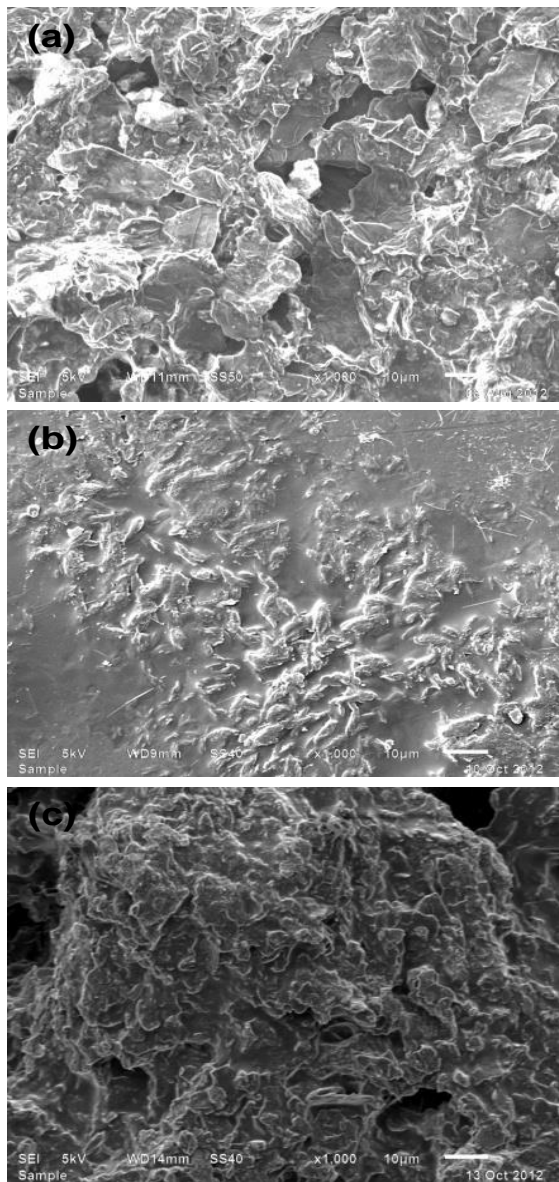


Fig. S1. represents the SEM image of a representative PGNCs synthesized at 9.0 %, w/w of graphene, the micrograph reveals a characteristic non-uniform distribution of the grains of PGNCs